nature human behaviour

Article

https://doi.org/10.1038/s41562-025-02362-8

Large-scale mega-analysis indicates that serial dependence deteriorates perceptual decision-making

Received: 12 February 2024

Accepted: 16 October 2025

Published online: 22 December 2025

Check for updates

Ayberk Ozkirli [1] ✉, Andrey Chetverikov [2] & David Pascucci [1,3,4]

For over a century, research has shown that human perceptual decisions are systematically influenced by prior perceptual experiences, a phenomenon known as serial dependence. It has recently been suggested that serial dependence can improve perceptual decision-making by mitigating uncertainty and reducing variability in perceptual estimates—leading to a superiority effect. However, this claim remains largely untested. Here we present a large-scale analysis, compiling the most extensive dataset of serial dependence studies from the past decade. Contrary to the proposed superiority effect, our findings indicate that serial dependence deteriorates rather than improves perceptual decision-making. These results challenge prevailing models and emphasize the need to rethink serial dependence and its role in human perception, cognition and behaviour.

Over the past decade, an unprecedented number of studies have investigated the phenomenon of serial dependence, in which human decisions are biased towards recent perceptual history[1–3]. Evident across a wide range of paradigms and stimuli, serial dependence has emerged as one of the most pervasive effects in human perception and cognition[4].

A classic example is the systematic bias observed in tasks where participants reproduce a basic feature of a visual stimulus, such as its orientation, across a series of trials. Participants' reports are attracted towards the feature of the stimulus shown on preceding trials—revealing a positive or attractive form of serial dependence that appears stable and reliable within individuals[2,5]. Strikingly, serial dependence extends beyond basic visual features such as orientation, colour and motion[1,6–13] to more complex and abstract judgements, including emotion[14,15], aesthetics[16], sense of agency[17] and even attractiveness in online dating[18]. This suggests that serial dependence is not merely a low-level perceptual bias but a fundamental aspect of brain function, pervasive across species and task domains[4,19,20].

The ubiquity of serial dependence has inspired novel computational models of perception and cognition[11,21–24] and motivated clinical research on its relevance in both typical and atypical brain function[25–27]. However, the mechanisms underlying serial dependence and its implications for perception remain debated[3]. Is serial dependence a bug or a feature? A prevailing view suggests that serial dependence serves a beneficial role: by integrating past and present stimuli, the perceptual system constructs a coherent and temporally smoothed representation of the world, reducing uncertainty and improving perceptual performance[22,28]. This idea is central to influential models of serial dependence—in particular, the cue integration[22] and Bayesian models[23,29].

These models, developed to explain the bias due to serial dependence, also predict clear effects on the variability of perceptual estimates, or error scatter. Specifically, when consecutive stimuli—such as orientations or motion directions—are highly similar, these models predict a decrease in error scatter (that is, more precise perceptual reports) compared with a hypothetical scenario without serial dependence (See 'Results' section for model predictions). We refer to this as a superiority effect[30], as performance improves due to serial dependence. However, this prediction remains largely untested.

While there is substantial evidence for systematic biases in perceptual judgements due to serial dependence, empirical support for

[1]Laboratory of Psychophysics, Brain Mind Institute, École Polytechnique Fédérale de Lausanne, Lausanne, Switzerland. [2]Department of Psychosocial Science, Faculty of Psychology, University of Bergen, Bergen, Norway. [3]Psychophysics and Neural Dynamics Lab, Radiology Department, Lausanne University Hospital and University of Lausanne, Lausanne, Switzerland. [4]The Sense Innovation and Research Center, Lausanne, Switzerland.
✉e-mail: ayberk.ozkirli@gmail.com

superiority effects is scarce, with only a few studies evaluating this phenomenon[22,29,31]. As research on serial dependence continues to grow and expand across domains, testing this key prediction is essential for understanding the true functional role of serial dependence in perception and cognition.

Here we tested the superiority effect by compiling the largest existing collection of datasets from the past decade, comprising 49 datasets from 22 studies[1,5,8–10,22,26,29,32–59] with more than half a million trials of orientation and motion direction reproduction tasks. In a targeted analysis, we tested whether human perceptual performance, quantified as the error scatter in reproduction responses, improves as a function of the similarity between consecutive visual stimuli, as predicted by the superiority effect. Specifically, we tested the prediction that perceptual precision should improve (that is, error scatter should be lower) when consecutive stimuli are similar compared with when they are highly dissimilar.

Contrary to the prevailing hypothesis, we found no evidence for a superiority effect. Instead, our results provided decisive evidence against it: perceptual precision remained comparable when consecutive stimuli were either identical or highly dissimilar, with a deterioration in between.

These findings challenge the notion that serial dependence is an unequivocally beneficial feature and call for a rethinking of its role in perception, cognition and behaviour. Furthermore, by compiling the largest dataset on serial dependence to date—including single-trial data in both raw and preprocessed formats using a standardized pipeline—this work provides an unprecedented resource for the research community to systematically test theoretical predictions, replicate findings and explore novel questions about the mechanisms and consequences of serial dependence.

Results

We analysed 49 datasets extracted from various experiments and conditions, involving 22 studies and more than half a million trials (Methods). The datasets included continuous reproduction tasks with orientation or motion stimuli (Fig. 1 and Table 1). In these tasks, observers were presented with a sequence of trials and asked to reproduce the relevant feature—orientation or motion direction—on each trial through adjustment responses.

Serial dependence was evident as a bias in adjustment errors towards the feature shown on the preceding trial, particularly for small absolute angular differences between current and previous stimuli ($|\Delta|$; Methods and Fig. 2). Despite variations in paradigms, stimuli and conditions, most datasets showed consistent positive serial dependence: adjustment errors were systematically biased towards the previous trial feature, with a positive effect across all datasets (mean, 1.06°; median, 0.99°). The error scatter, quantified as the overall standard deviation of adjustment errors (Fig. 1c), varied substantially across datasets (Fig. 2).

According to the hypothesis that serial dependence enhances perceptual performance, leading to a superiority effect, performance should improve and error scatter should decrease when $|\Delta|$ between the current and previous stimuli is small or zero (that is, when the stimuli are highly similar). Figure 3a illustrates explicit examples of this predicted pattern, derived from simulated data based on the cue integration and Bayesian models at varying levels of overall scatter. In both models, the current and previous stimuli are integrated while accounting for the uncertainty in their perceptual representations, albeit through different computational principles (see 'Reference models' in Supplementary Information).

As shown, both models predict the characteristic bias pattern observed in many studies[2,3] but also a specific effect on scatter: error scatter decreases below the baseline imposed in the simulations, as the similarity between the current and previous stimuli increases (Methods). In particular, both models predict higher precision

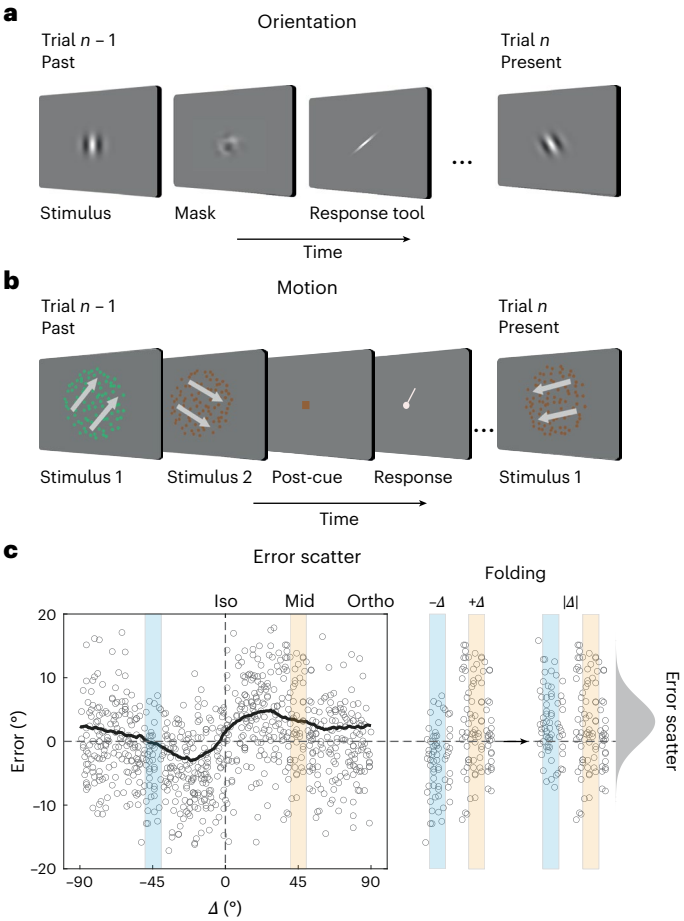

Fig. 1 | Experimental paradigms and serial dependence. a,**b**, Illustration of two widely used paradigms: orientation reproduction tasks (**a**) and motion direction reproduction tasks (**b**). In orientation tasks, participants reproduced the perceived tilt of a Gabor patch using a circular response tool. In some datasets, a mask was presented after the stimulus to minimize after-effects. In motion direction tasks, participants reported the perceived direction of motion using a response tool rotating within a 360° circular space. Panel **b** illustrates a post-cueing paradigm adapted from ref. 9 (Experiments 1–2). A summary of the paradigms is provided in Table 1, with further details available in the referenced studies. **c**, Error distribution for an example subject in an orientation task. Single-trial errors are plotted against the difference between the target feature (for example, orientation) in two consecutive trials (Δ, past minus present, in degrees). The plot exhibits a typical attractive bias towards the past, with positive errors when Δ is positive and negative errors when Δ is negative, particularly for small Δ values. The labels 'Iso', 'Mid' and 'Ortho' indicate error distributions when the difference between the current and prior stimulus orientations is 0° (iso), 45° (mid) or 90° (ortho). The plot also illustrates the process of error folding, in which errors for negative Δ values (highlighted in blue) are flipped in sign and combined with their corresponding positive Δ values (in orange). This procedure helps characterize the error distribution in the presence of bias (see Methods for details). The error scatter, defined as the standard deviation of the folded error distribution (shown in grey), is then computed under the assumption that errors are symmetrically distributed around $\Delta = 0°$.

(that is, lower scatter) in the iso condition ($|\Delta| = 0°$) than in the mid ($|\Delta| = 45°$) and ortho ($|\Delta| = 90°$) conditions—an effect that would not be observed in the absence of serial dependence.

To test for superiority effects in empirical data, we first modelled the error scatter as a function of $|\Delta|$, using a weighted, flexible-degree polynomial fit at the individual grouping level (Methods). Stimulus-specific biases were removed prior to modelling to prevent critical confounds (see 'Confounding effect of stimulus-specific biases' in Supplementary Information). The pattern clearly revealed

https://doi.org/10.1038/s41562-025-02362-8

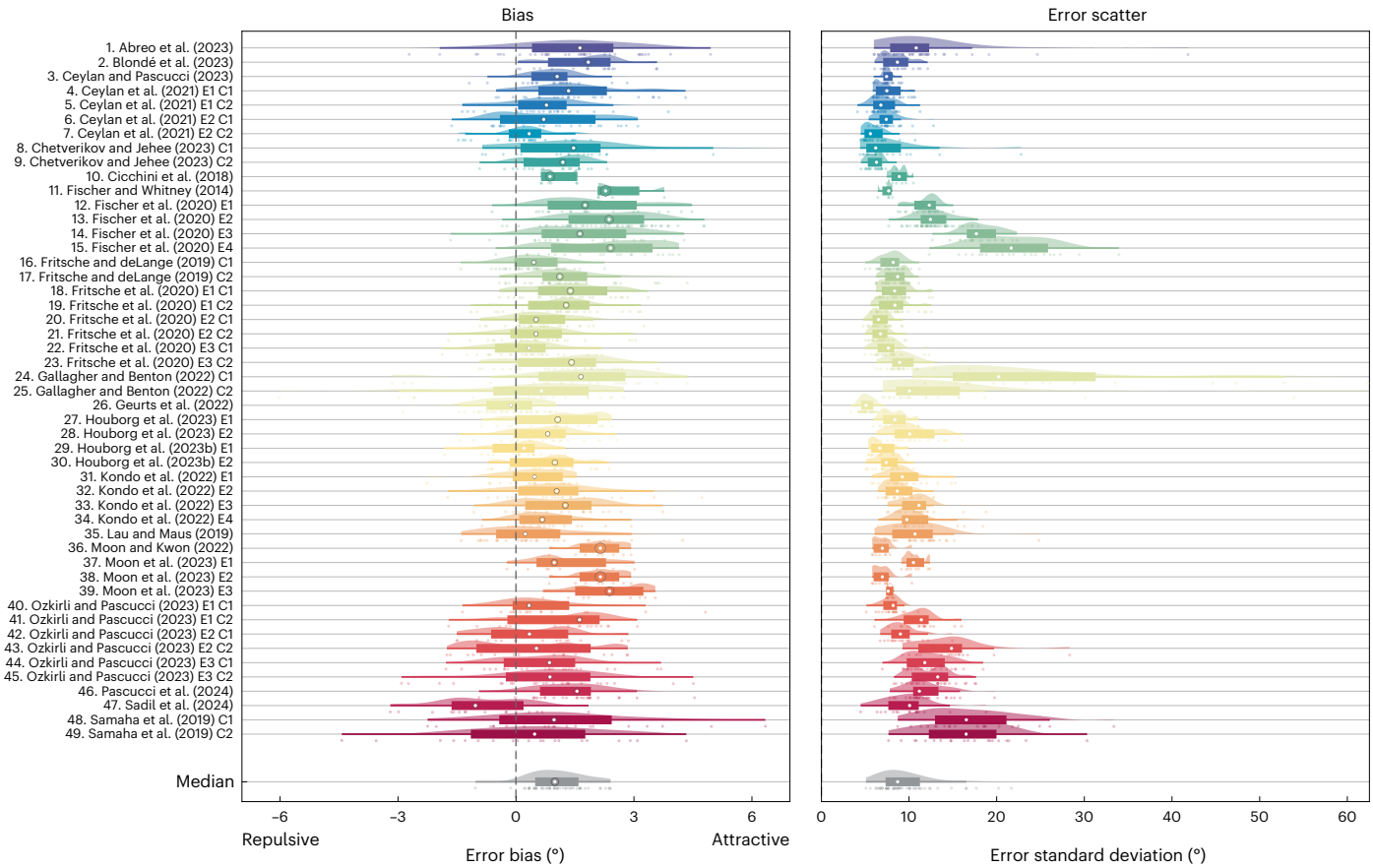

Fig. 2 | Summary of bias and error scatter across 49 datasets. The bias (left) is computed as the average folded error within the 0–45° $|\Delta|$ range (Methods). Positive values indicate an attractive bias towards the previous trial's orientation or motion direction, while negative values indicate a repulsive bias away from it. The error scatter (right) is quantified as the overall standard deviation of reproduction errors (*x* axis). The *y* axis lists the datasets, with the median across all datasets shown at the bottom (grey box plots and distributions). Each dataset is visualized using box plots overlaid on individual participant distributions, with dots representing individual subject values. In the median plot at the bottom, each dot represents the average bias of a dataset. In the bias plot (left), the central white circles, positioned at the median of each distribution, represent the reference effect size ($g = 0.2$). The surrounding coloured circles, outlined in black, indicate the effect size of each dataset relative to this reference. In the error scatter plot (right), the white dots mark the median value for each dataset. In the box plots, the lower and upper edges of the box correspond to the 25th and 75th percentiles, and the whiskers extend to the most extreme values within 1.5 times the interquartile range from the upper and lower quartiles. The violin plots represent the distribution of the data using a kernel density estimate.

an inverted U-shaped relationship, with error scatter increasing for intermediate $|\Delta|$ and decreasing again for larger $|\Delta|$ values (Fig. 3b).

We then evaluated differences in the error scatter magnitude estimated with the polynomial fit at the three key $|\Delta|$ values using a linear mixed-effects model (LMM). The fixed effect in the model was a categorical predictor with the three angular differences iso, mid and ortho. The LMM accounted for random effects at multiple hierarchical levels, including participants, datasets and their nested interactions (see Methods for a detailed description).

The fixed-effect estimates revealed a significant increase in error scatter from iso to mid ($t_{2988} = 8.62$, $P < 0.001$). However, no significant difference was observed between iso and ortho ($t_{2988} = 0.36$, $P = 0.717$), indicating comparable error scatter (Fig. 4). Importantly, while heterogeneity in error scatter at iso was substantial across observers and experiments, the relative modulation by stimulus similarity (that is, differences between iso and mid and between iso and ortho) was highly consistent (see 'Assessing heterogeneity in LMM results' in Supplementary Information), and the overall pattern was comparable between orientation and motion stimuli (Supplementary Fig. 7).

To further evaluate these findings, we fit a second, reduced LMM by merging the iso and ortho categories. A Bayesian information criterion (BIC) comparison between the full and reduced models yielded a ΔBIC of −67.84, resulting in a Bayes factor ($BF_{\text{reduced over full}}$) of >100 in favour of the reduced model. This provides decisive evidence against the existence of a superiority effect due to serial dependence. That is, error scatter was comparable whether the current and previous stimuli were identical (iso) or differed by 90° (ortho).

These findings were further validated using a non-parametric binning approach (see 'Control analysis' in Supplementary Information). Note that the two reference models, the cue integration and Bayesian models, always predict a reduction of the error scatter in the iso compared with the ortho condition, thus predicting a pattern incompatible with our findings (Fig. 3a).

Discussion

Serial dependence is a pervasive aspect of human behaviour and has become an expanding field of research in recent years. Emerging perspectives suggest that integrating past and present sensory information serves a functional role by reducing the variability of perceptual estimates when consecutive stimuli are similar, leading to a superiority effect—that is, enhanced perceptual precision[22,28]. In this study, we tested this hypothesis using the largest collection of single-trial data employed in serial dependence research over the past decade. We analysed 49 datasets, comprising over half a million trials, using standardized procedures while controlling for potential confounds. Contrary to the predicted superiority effect,

https://doi.org/10.1038/s41562-025-02362-8

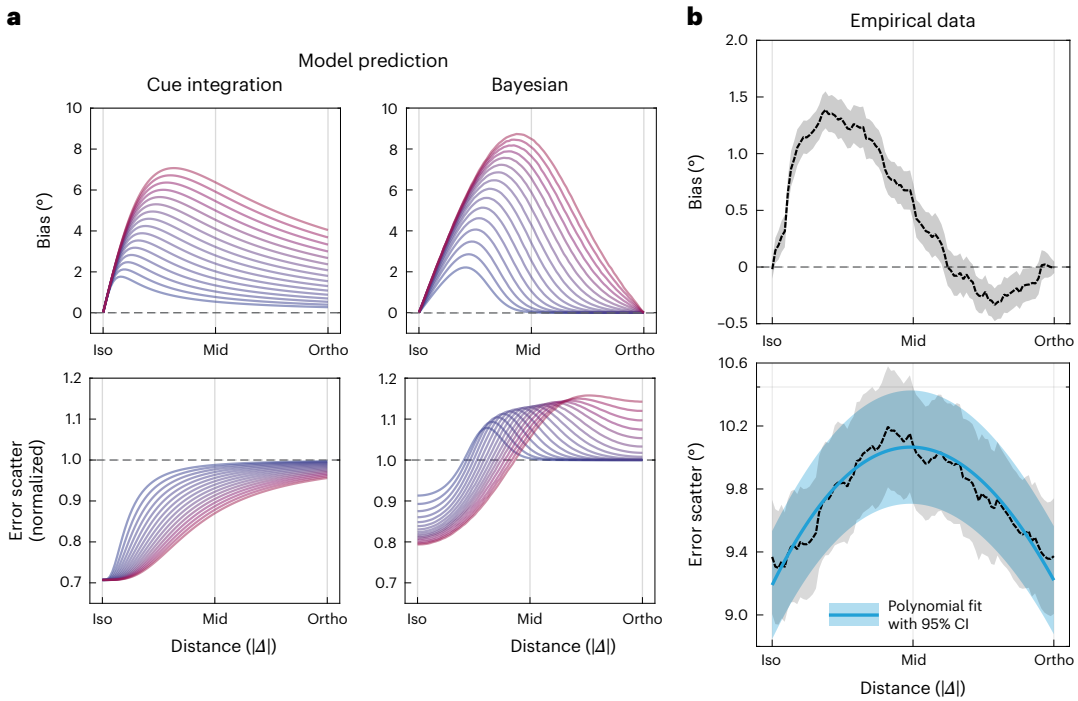

Fig. 3 | Bias and error scatter as functions of |Δ| in model predictions and empirical data. a, Predictions from two models of serial dependence (see 'Reference models' in Supplementary Information for detailed formulations): the cue integration model (first column) and the Bayesian model (second column), showing bias (first row) and error scatter (second row) as functions of |Δ|. The three key angular differences analysed (iso, mid and ortho) are marked on the *x* axis. The colour gradient from dark to light violet represents simulations with increasing baseline scatter (see 'Reference models' in Supplementary Information), ranging from 5° to 20°, respectively. In the bias plots (first row), positive values on the *y* axis indicate attraction towards the previous stimulus feature. In the scatter plots (second row), the *y* axis represents error scatter normalized to the baseline level (that is, the baseline scatter imposed in each simulation (Supplementary Information), here highlighted by the dashed black line). Note that we simulated a broad range of baseline scatter values to show that, regardless of the value simulated, the error scatter at iso is always predicted to be smaller than that in the ortho condition for both models. **b**, Empirical results from 49 datasets, showing bias (top) and error scatter (bottom) as functions of |Δ|. The black lines represent average smoothed data across all grouping levels, using a kernel of 11° for both bias and scatter. The shaded areas represent 95% confidence intervals (CIs). In the error scatter plot, the blue line and shaded intervals represent estimations from the best-fitting polynomial model (Methods and Results).

our results provide no evidence that serial dependence improves perceptual precision. Instead, our findings suggest a detrimental effect on perceptual performance.

We investigated how serial dependence influences error scatter, an inverse measure of perceptual precision, in orientation and motion direction reproduction tasks—two of the most widely used paradigms in the field[3]. Specifically, we compared error scatter across three key angular differences between consecutive stimuli: iso (identical stimuli), mid (45° difference) and ortho (90° difference). If serial dependence indeed enhances perceptual precision, error scatter should be the lowest in the iso condition, where current and previous stimuli are identical[22,29]. However, we found comparable error scatter between the iso condition (that is, when consecutive stimuli were identical) and ortho condition (that is, when stimulus differences were maximal), with an increase at intermediate differences (mid condition).

This pattern deviates in a crucial way from predictions made by the dominant normative models of serial dependence, including cue integration and Bayesian frameworks[22,23,29,31]. These models assume that recent perceptual history acts as a prior, combining with current sensory evidence to minimize uncertainty. Consequently, they predict the lowest error scatter when past and present stimuli strongly overlap (for example, at iso), with larger error scatter at greater angular differences (for example, at the mid and ortho conditions).

Although the models differ in their specific predictions about the shape of this pattern (Fig. 3a), none predict that error scatter at the ortho distance will be comparable to that at the iso distance. Rather, they assume that as stimuli become more dissimilar, the influence of serial dependence weakens[2,3], and performance approaches baseline levels where serial dependence has little to no effect. Thus, these models and the related views predict always lower error scatter in the iso condition than in the ortho condition. Our results from this large-scale analysis, however, clearly contradict these predictions: error scatter remained comparable between the iso and ortho conditions.

While our study systematically assesses the effects of serial dependence on error scatter in a large sample of datasets, there have been a few previous attempts to investigate these effects on single studies[22,29,31,60,61]. For instance, in Fritsche et al.[29] (datasets 18–23), two out of three experiments qualitatively supported superiority effects, while the third resembled the overall pattern observed here. In the Supplementary Information, we show that such superiority-like patterns emerge spuriously from interactions between stimulus-specific biases and angular differences between current and previous stimuli. If uncorrected, these biases introduce systematic variance in reproduction errors, confounding estimates of error scatter and its true relation with serial dependence, eventually leading to artificial differences between iso and ortho conditions (see 'Confounding effect of stimulus-specific biases' in Supplementary Information). Across several control analyses, we show that these stimulus-specific modulations—previously unknown and overlooked in earlier work—are unrelated to classic serial dependence effects (Supplementary Fig. 5b) and may represent a distinct form of history dependence that warrants dedicated investigation. After we controlled for this confound, both the artificial increase in overall error scatter and the apparent superiority effects largely

https://doi.org/10.1038/s41562-025-02362-8

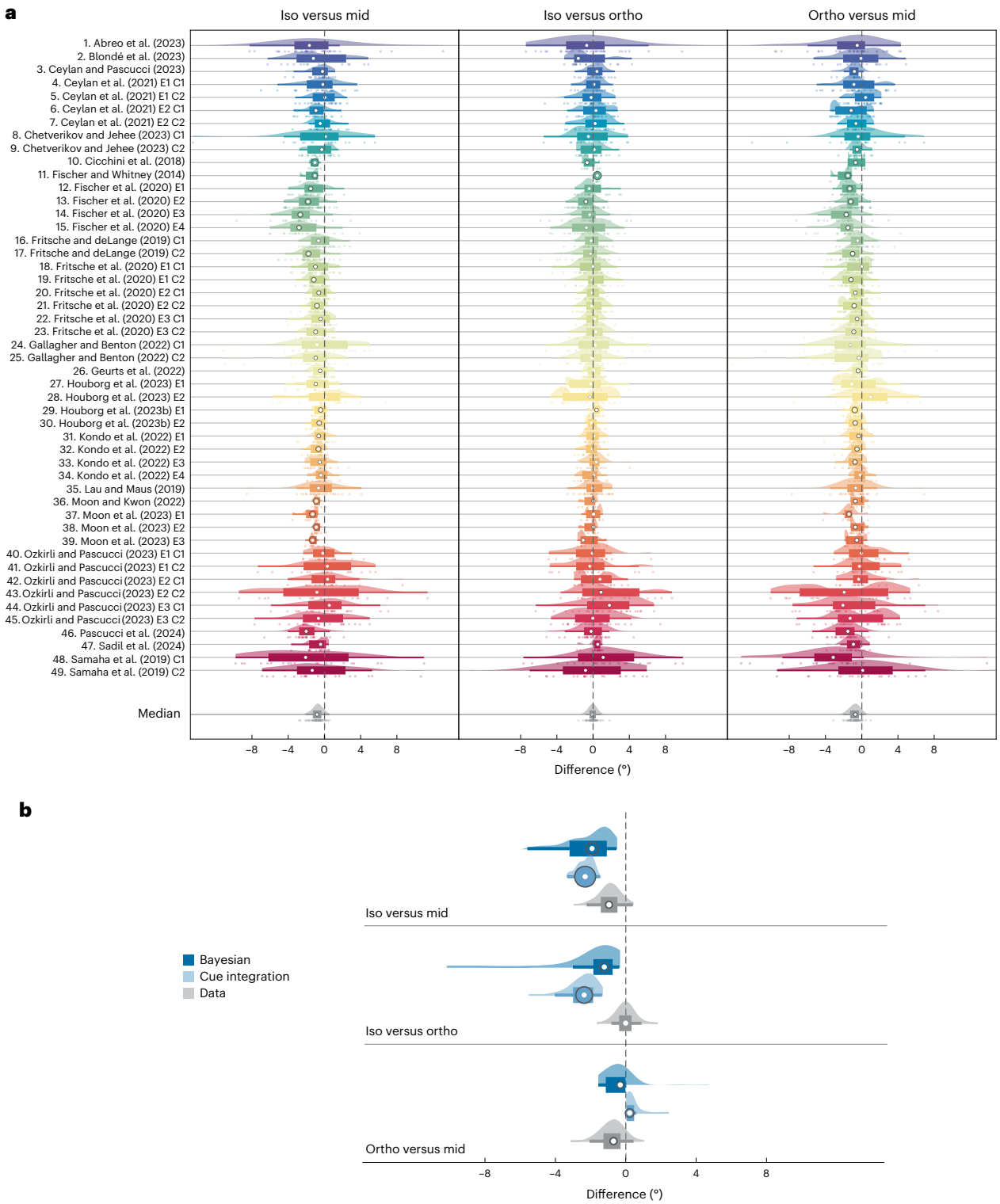

Fig. 4 | Pairwise comparisons of error scatter across conditions and model predictions. a, Observed differences in error scatter for each dataset and each pairwise comparison (iso–mid, iso–ortho and ortho–mid), alongside model predictions based on the median scatter across the 49 datasets. The box plots illustrate the distribution of participant-level differences for each comparison within each dataset (first 49 rows) and the median distribution across all datasets (final row). In each row, the central white circle, positioned at the median of the distribution, represents the reference effect size ($g = 0.2$). The surrounding coloured circle, outlined in black, indicates the effect size of each dataset relative to this reference. Two-tailed paired *t*-tests showed that the median error scatters of datasets were significantly different between iso and mid ($t_{48} = -8.3$, $P < 0.001$) and between ortho and mid ($t_{48} = -8.27$, $P < 0.001$), but not between iso and ortho ($t_{48} = -0.52$, $P = 0.606$). **b**, Summary of the observed pattern, showing the distribution of median values from the empirical data ($N = 49$, grey) compared to model predictions (Bayesian model in dark blue, cue integration model in light blue). The grey box plots in this panel provide a zoomed-in view of the final rows from **a**. In the box plots in both panels, the lower and upper edges of the box correspond to the 25th and 75th percentiles, and the whiskers extend to the most extreme values within 1.5 times the interquartile range from the upper and lower quartiles. The violin plots represent the distribution of the data using a kernel density estimate.

disappeared across datasets, including those from Fritsche et al.[29] (Supplementary Fig. 2).

Despite our approach to removing confounds and standardizing preprocessing, we cannot rule out the possibility that subtle superiority effects exist or may be better revealed with paradigms other than reproduction tasks[60]. However, any such effect, if existing, must be extremely small compared with the dominant pattern: a robust increase in error scatter at intermediate angular differences (the mid condition). This finding, not fully captured by existing models, underscores the need for revised theoretical accounts of how serial dependence influences the variability of perceptual estimates.

What could explain comparable performance when consecutive stimuli either maintain or break continuity? One possibility is the interplay between attractive and repulsive serial dependence effects, which have been proposed as competing mechanisms at different processing levels[11,31,62]. Repulsive effects, often observed as negative deflections at the tails of the serial dependence bias function (Fig. 3b, top), are typically attributed to low-level adaptation mechanisms[11,31]. Such mechanisms have been linked to enhanced neuronal selectivity at orthogonal orientations following brief adaptation[63], which in turn could influence perceptual precision. However, to our knowledge, no studies have demonstrated that repulsive serial dependence effects selectively reduce error scatter for large stimulus differences, at least within the paradigms commonly used. Moreover, the studies analysed here were designed to enhance attractive serial dependence while minimizing adaptation and repulsive effects (for example, through brief, low-contrast stimuli and noise masks).

Instead, we propose that the error scatter pattern reflects interference from contextual stimuli, a phenomenon widely observed in spatial vision[30,64,65] and working memory[66,67]. In this framework, the representation of the current stimulus results from a superposition of the actual stimulus and contextual influences. When consecutive stimuli share identical features, interference is minimal, because their representations fully overlap. However, as differences in stimulus features increase, interference distorts the representation, leading to larger errors. This interpretation aligns with our results, particularly if interference effects diminish when stimuli become highly discernible, producing comparable performance in the iso and ortho conditions. In the context of serial dependence, this suggests that lingering traces of previous stimuli impair rather than enhance perceptual estimates by interfering with current representations.

This account implies fundamentally different effects and mechanisms than those proposed by accounts predicting a superiority effect. While we highlight interference as a plausible alternative explanation, the main purpose of this work was the mega-analysis itself, rather than advocating for a new model. Future studies will be needed to determine whether the observed error scatter patterns are better explained by the coexistence of two distinct beneficial mechanisms—one attractive at iso and the other repulsive at ortho—or, more parsimoniously, by interference effects that scale with stimulus dissimilarity.

Our findings also relate to broader frameworks linking the effects of temporal and spatial context under a shared computational mechanism[68]. These frameworks suggest that contextual integration—whether across time (serial dependence) or space (visual crowding)—aims to minimize uncertainty. A recent study on visual crowding, for instance, reported that flankers iso-oriented to a target reduced error scatter compared with orthogonal target-flanker orientations or a target-only condition[69]. However, a replication study failed to find such superiority effects, instead revealing comparable error scatter for iso and ortho flankers, closely mirroring the pattern observed in our serial dependence study[30]. This result is consistent with prior reports in the crowding literature[70–73]. Notably, in spatial crowding studies, a clear baseline can be established by measuring error scatter in the absence of flankers, making it easier to isolate contextual effects. Thus, our findings, together with recent results in visual crowding, suggest that error scatter—and therefore the precision of perceptual estimates—is comparable when contextual stimuli are either highly similar or highly dissimilar to the target stimulus, challenging the assumption that perceptual precision necessarily benefits from contextual effects.

We propose that interference should be considered a viable alternative to existing models, offering a parsimonious explanation for the observed deviations from normative predictions. However, other novel or existing models—such as those based on working memory dynamics or entanglement of sensory signals[24,74]—should be evaluated against existing frameworks to determine which best accounts for the error scatter pattern observed in our study. This does not imply that integrating past and present sensory information is universally detrimental—perceptual continuity and stability remain key adaptive functions of the brain[28]. Nor do we claim that Bayesian and cue integration models are fundamentally incorrect. The ability to integrate multiple sources of information is a core function of the brain, and these models provide valuable predictive frameworks[75]. However, in the context of classic serial dependence paradigms, where stimuli are randomized and independent across trials, there is no functional advantage to combining past and present sensory inputs. If traces of prior stimuli persist, it is plausible that they interfere with current perceptual decisions and thus deteriorate performance.

Conversely, the amount of interference may be decreased when stimuli are temporally correlated. If serial dependence were an adaptive mechanism, one would expect it to be strongest under conditions of temporal regularity. Paradoxically, however, studies introducing temporal correlations in stimulus sequences have reported weak serial dependence effects[60], or even a reduction in serial dependence relative to uncorrelated sequences, and stronger repulsive biases of stimulus history[34,76]. This apparent paradox closely parallels effects observed in spatial vision: in visual crowding, interference from flankers in target recognition is reduced when flankers form a coherent spatial configuration—a phenomenon known as uncrowding[64,77]. Crucially, however, performance in crowding and uncrowding is never superior to baseline performance with the target alone[30]. The pattern of error scatter reported here suggests that an analogous form of interference—one that current models fail to capture—is also at play in serial dependence.

In sum, our findings impose important constraints on broad claims about the role of serial dependence across different tasks and processing domains. We provide strong evidence against the idea that serial dependence enhances perceptual precision. Instead, our results suggest that serial dependence may be better explained as a form of interference, which increases response variability rather than reducing it. These findings challenge prevailing theories and call for a conceptual and computational reassessment of serial dependence. To support this, we provide an open-access, automated analysis pipeline, enabling researchers to contribute additional datasets and expand a continuously growing large-scale analysis of serial dependence. This open framework will allow for systematic testing of alternative models, fostering a more comprehensive understanding of how perceptual history shapes behaviour.

Methods

Dataset selection and exclusion criteria

We conducted a search on PubMed using the keyword 'serial dependence' for studies published between 2014 (from the initial study of Fischer and Whitney[1]) and 2024. Studies were selected on the basis of the following criteria:

(1) Single-trial data publicly available online
(2) Adjustment tasks involving orientation or motion stimuli with circular responses (for example, participants reproducing the orientation of a Gabor patch or the motion direction of dot clouds)

https://doi.org/10.1038/s41562-025-02362-8

Table 1 | The summary of datasets included in the final analysis, listed alphabetically

ID	Study	Reproduce	Datasets	*N*	All trials	Clean trials
1	Abreo et al.[32,33]	Orientation	1	36	6,754	6,335
2	Blondé et al.[34,35]	Orientation	1	17	2,380	2,228
3	Ceylan and Pascucci[36]*	Orientation	1	20	6,000	5,822
4	Ceylan et al.[8,37]	Orientation	4	48	19,200	18,662
5	Chetverikov and Jehee[38,39]	Motion	2	18	19,836	8,389
6	Cicchini et al.[22,40]	Orientation	1	6	12,300	11,833
7	Fischer and Whitney[1]*	Orientation	1	4	3,328	3,197
8	Fischer et al.[9,41]	Motion	4	109	176,256	86,343
9	Fritsche and de Lange[42]	Orientation	2	34	19,584	19,089
10	Fritsche et al.[29]	Orientation	6	71	67,148	65,197
11	Gallagher and Benton[43,44]	Orientation	2	20	16,420	15,899
12	Geurts et al.[45]	Orientation	1	32	15,520	14,854
13	Houborg et al.[46]*	Orientation	2	31	6,200	5,852
14	Houborg et al.[47,59]	Orientation	2	32	31,720	31,168
15	Kondo et al.[5]*	Orientation	4	76	76,000	73,234
16	Lau and Maus[48,49]	Orientation	1	29	15,404	13,732
17	Moon and Kwon[10,50]	Motion	1	8	13,170	6,792
18	Moon et al.[51,52]	Motion	3	24	39,330	20,466
19	Ozkirli and Pascucci[53,54]	Orientation	6	56	22,328	21,622
20	Pascucci et al.[26,55]	Orientation	1	26	20,800	13,512
21	Sadil et al.[56]*	Orientation	1	16	24,240	23,537
22	Samaha et al.[57,58]	Orientation	2	20	5,930	5,501
		Total	49	733	619,848	473,264

The analysis included 22 studies, many of which featured multiple experiments and repeated-measures designs with multiple conditions. These were preprocessed separately, resulting in 49 datasets, 733 globally unique participants and a total of 619,848 trials. After data cleaning and restricting of the angular difference ($|\Delta|$) to ≤90°, 473,264 trials remained. Motion datasets had a notable reduction in trial counts due to this restriction. *Data received through communication with the original authors.

(3) Trial-by-trial orientation or motion direction changes (Δ) covering 0° to ±90°, using uniform or randomly determined trial-by-trial changes in Δ.

From the 198 studies identified in the search, 20 met these criteria (highlighted in orange in Supplementary Table 1). However, because the dataset from ref. 29 overlapped with that from ref. 62, the final count from the database effectively comprised 19 unique studies. Additionally, three studies that satisfied the inclusion criteria but were not part of the PubMed search results were included[38,45,53], resulting in 22 studies in total.

The selected studies are summarized in Table 1, along with key information (for detailed descriptions of each task and apparatus, please refer to the original studies). Of the 22 studies included, several featured multiple experiments and repeated-measures designs with various conditions. To account for the potential influence of these conditions on the strength of serial dependence and error scatter, each experiment and within-experiment condition was treated as a separate dataset. This resulted in a total of 49 datasets, comprising 733 participants and 619,848 trials.

Data preprocessing

Data processing was done by using MATLAB v.2023b[78]. To ensure consistency in the analysis pipeline, we applied a standardized, minimum data-cleaning procedure to all datasets. It is important to note that this procedure, along with the resulting estimates, may differ from those used in the original studies.

The preprocessing involved two key steps: removing outliers and correcting for stimulus-specific bias (for example, non-uniform error distribution across orientations or motion directions). Below, we outline the rationale and approach used for each step.

Removal of outliers. Outlier errors can compromise estimates of serial dependence effects, in terms of both bias and variability[57]. Several approaches to outlier removal have been previously used, such as excluding errors above or below an arbitrary threshold or removing values that deviate by a certain number of standard deviations from the mean (typically three standard deviations)[29]. Here we adopted a two-stage non-parametric approach based on quartiles and the interquartile range, opting for a robust, assumption-free method.

First, we marked as outliers all absolute errors greater than 90°. This step was applied only to datasets involving motion direction judgements, where errors exceeding 90° indicated reports of the orthogonal or opposite motion direction. This helped avoid interpretational issues in cases where participants may have confused opposite motion directions. In orientation tasks, errors were already constrained to a maximum of 90° due to the circular nature of the 0–179° scale, with errors calculated as the acute angle. Additionally, trials with adjustment times (when available) exceeding 10 seconds were excluded.

In the second stage, we used the MATLAB isoutlier function with the 'quartiles' method. This approach identifies outliers as any errors more than 1.5 interquartile ranges above the upper quartile or below the lower quartile. This procedure was applied separately for each participant, experiment and condition. Only trials with $|\Delta| \leq 90°$ that were not identified as outliers in either of the two stages were included in the subsequent analyses. This choice was motivated by the fact that judgements regarding motion directions that differ by 180° can be influenced by the orientation information contained in motion streaks[6,38,51,79], introducing potential confounds where 0° and 180° might be represented in a similar, rather than orthogonal, way.

Removal of stimulus-specific biases. Adjustment responses with circular features (for example, orientation or motion direction) are systematically affected by stimulus-specific biases, where errors are non-uniformly distributed around the actual stimulus values. These biases often manifest as deviations away from cardinal directions and toward oblique angles. While such stimulus-specific biases are typically considered independent of serial dependence effects, they introduce additional variance in the error distribution. To address this, several studies have employed techniques that remove these biases, such as fitting polynomial or sinusoidal functions to the error as a function of the stimulus angle and using the residuals for further analysis[11,23,46,80].

Here we used a similar residualization approach while accounting for the circular nature of the stimuli in orientation and motion direction tasks. Specifically, we fitted the errors with a circular-linear model, using a set of periodic basis functions defined by the sine and cosine of the stimulus angle presented on each trial, up to the sixth harmonic. This set of periodic predictors, along with an intercept to

account for any systematic bias in reporting features as more clockwise or counterclockwise, was fitted to the errors using ordinary least squares regression via the pseudoinverse. The pseudoinverse ensured numerical stability and minimized the issue of multicollinearity. This approach effectively removed periodic stimulus-specific biases (Supplementary Fig. 1) and helped avoid drastic confounds in the estimation of the error scatter (Supplementary Figs. 3 and 4). As an alternative approach, we also used the circhelp package in R[81,82] to remove orientation bias confounds from each dataset, obtaining fully comparable results (not shown).

Modelling the error scatter. As described above, the data were first restricted to trials with $|\Delta| \leq 90°$ that were not classified as outliers (76% of all trials). Since serial dependence effects are generally symmetric for negative and positive Δ (previous minus current orientation), we applied a folding approach[7,23,46]. This method involved flipping the sign of errors associated with negative Δ values to align them with their corresponding positive Δ values (Fig. 1c). This folding approach removed the influence of the serial dependence bias in the estimate of error scatter, while also doubling the number of data points per $|\Delta|$ and increasing the robustness of error scatter estimation.

After the folding step, the error scatter for each $|\Delta|$ available for that participant and condition was calculated as the standard deviation of the errors within that $|\Delta|$. Any $|\Delta|$ with only one trial was excluded from further analysis, as its standard deviation would be zero. The relationship between error scatter and $|\Delta|$ was then modelled using polynomial fits, conducted separately at the level of experiment–participant–condition (that is, grouping level). Second- and third-degree polynomial models were tested for each of the 1,000 grouping levels independently.

We used a weighted polynomial model, with $|\Delta|$ values weighted as a function of the number of trials in each $|\Delta|$. Across all grouping levels, the number of trials per $|\Delta|$ within a level ranged from 2 to 401 (median, 5 trials). As small trial counts may introduce noise in standard deviation estimates, these cases were downweighed in the model fitting. This approach avoided binning or applying moving averages over the $|\Delta|$ values, thereby preserving a high resolution across the 0–90° angular difference space.

To evaluate the quality of polynomial fits with different degrees, we computed the BIC for each tested polynomial-degree model separately for each grouping level (2 × 1,000 times). First, the residuals were calculated as the difference between the observed scatter values and the predicted values from the polynomial fit. The sum of squared residuals (SSR) was calculated by first weighing the residuals by the number of trials for each $|\Delta|$. The BIC was then calculated using the formula:

$$\mathrm{BIC} = n \times \log\left(\frac{\mathrm{SSR}}{n}\right) + k \times \log(n) \quad (1)$$

where n is the number of $|\Delta|$ values, at a certain grouping level, for which more than one trial is available, and k is the number of model parameters (equal to the polynomial degree plus one for the intercept). The BIC was used to balance model complexity and goodness of fit, penalizing overly complex models. To select the optimal polynomial degree for each grouping level, we calculated the BIC for second- and third-degree polynomial fits and chose the degree with the lowest BIC. If the second-degree fit satisfied the condition $\mathrm{BIC}_2 \leq \mathrm{BIC}_3 + 2$, the second degree was selected as the optimal fit.

The final best-fit polynomial at each grouping level, mostly a second-degree polynomial (for 953 levels out of 1,000), was then evaluated across the full $|\Delta|$ range (0–90°). Three fits producing unrealistic (for example, negative) scatter values were excluded from further analysis. This procedure yielded estimates of error scatter as a function of $|\Delta|$ for each grouping level, enabling robust comparison of scatter trends within and across datasets.

Following the main objective of the study—whether serial dependence improves performance by reducing error scatter for highly similar compared with dissimilar stimuli—we extracted model predictions at three specific points along the $|\Delta|$ axis: iso ($|\Delta| = 0°$), fully identical consecutive stimuli; mid ($|\Delta| = 45°$), intermediate stimulus difference; and ortho ($|\Delta| = 90°$), maximally different stimuli. The advantage of the polynomial fitting approach is that it allowed us to robustly estimate the error scatter at these critical points, for which the number of available trials can be low in some cases, by using information from all available data (from $|\Delta| = 0°$ to 90°). The estimated values of error scatter at these three critical points were then submitted to further statistical analysis (see 'LMM' below; and 'Control analysis' in Supplementary Information for the validation of polynomial estimates using a model-free approach).

The logic of our analysis rests on the well-established assumption that, for attractive forms of serial dependence, orthogonal stimuli (ortho) lie outside the range of the effect[2] and therefore provide the most appropriate reference for testing superiority effects. These effects, if present, should specifically arise from attractive serial dependence at small orientation differences, with the strongest impact expected at the iso level. Indeed, the models considered here consistently predict a difference between iso and ortho, with the ortho level approximating the 'baseline' condition of no attractive serial dependence (Fig. 3a).

LMM

We implemented an LMM in MATLAB using the fitlme function. The dependent variable was the predicted error scatter (ES) (see 'Modelling the error scatter'), and the fixed effect was a categorical predictor representing the three levels of stimulus differences defined above (iso, mid and ortho), which we refer to as the similarity index (SI).

To account for variability at multiple nested levels, we specified a maximal random-effects structure, including dataset-level variability (random effect: codenum), participant-level variability (random effect: obsid) and repeated measurements within participants across conditions (random effect: codenum:obsid). All random effects included both an intercept and a random slope for the effect of SI. The model formula was:

$$\mathrm{ES} \sim \mathrm{SI} + (1 + \mathrm{SI}|\mathrm{obsid}) + (1 + \mathrm{SI}|\mathrm{codenum}) + (1 + \mathrm{SI}|\mathrm{codenum} : \mathrm{obsid}) \quad (2)$$

The fixed effects of interest included the intercept, representing the level of scatter in the iso condition (where the previous and current stimuli were identical), and the two coefficients quantifying the differences in scatter between iso and mid and between iso and ortho.

To assess the significance of including the full SI (iso, mid and ortho) as a fixed effect, we compared the full model to a reduced model. In the reduced model, the SI was replaced with a simplified categorical variable (SIr) with fewer levels, specifically recoding iso as identical to ortho, resulting in two categories instead of three. The reduced model formula was:

$$\mathrm{ES} \sim \mathrm{SIr} + (1 + \mathrm{SIr}|\mathrm{obsid}) + (1 + \mathrm{SIr}|\mathrm{codenum}) + (1 + \mathrm{SIr}|\mathrm{codenum} : \mathrm{obsid}) \quad (3)$$

Both the full and reduced models were fit using the fitlme function, and their BIC values were extracted. The difference in BIC (ΔBIC) between the reduced and full models was calculated as:

$$\Delta\mathrm{BIC} = \mathrm{BIC}_{\mathrm{reduced}} - \mathrm{BIC}_{\mathrm{full}} \quad (4)$$

where a lower BIC value indicates a better-fitting model after accounting for model complexity. To quantify the relative evidence in favour

of the reduced model compared with the full model, the Bayes factor was calculated using the formula:

$$\mathrm{BF}_{\text{reduced over full}} = \frac{1}{e^{\Delta \mathrm{BIC}/2}} \quad (5)$$

A ΔBIC > 0 and $\mathrm{BF}_{\text{reduced over full}} < 1$ provide evidence in favour of the full model, indicating a significant difference in error scatter between the iso and ortho levels. Conversely, a ΔBIC < 0 and $\mathrm{BF}_{\text{reduced over full}} > 1$ suggest that the reduced model provides a better fit, implying that error scatter at the iso and ortho levels is comparable.

Reporting summary

Further information on research design is available in the Nature Portfolio Reporting Summary linked to this article.

Data availability

The datasets containing standardized raw data for the mega-analysis are available at https://github.com/aozkirli/Large-scale-mega-analysis-on-serial-dependence/tree/main. The use of any part of this compiled dataset in future studies requires citation of both this publication and the original source studies from which the data were obtained.

Code availability

The analysis code can be found at https://github.com/aozkirli/Large-scale-mega-analysis-on-serial-dependence/tree/main.

References

1. Fischer, J. & Whitney, D. Serial dependence in visual perception. *Nat. Neurosci.* **17**, 738–743 (2014).
2. Manassi, M., Murai, Y. & Whitney, D. Serial dependence in visual perception: a meta-analysis and review. *J. Vis.* **23**, 18 (2023).
3. Pascucci, D. et al. Serial dependence in visual perception: a review. *J. Vis.* **23**, 9 (2023).
4. Kiyonaga, A., Scimeca, J. M., Bliss, D. P. & Whitney, D. Serial dependence across perception, attention, and memory. *Trends Cogn. Sci.* **21**, 493–497 (2017).
5. Kondo, A., Murai, Y. & Whitney, D. The test–retest reliability and spatial tuning of serial dependence in orientation perception. *J. Vis.* **22**, 5 (2022).
6. Alais, D., Leung, J. & Van der Burg, E. Linear summation of repulsive and attractive serial dependencies: orientation and motion dependencies sum in motion perception. *J. Neurosci.* **37**, 4381–4390 (2017).
7. Barbosa, J. & Compte, A. Build-up of serial dependence in color working memory. *Sci. Rep.* **10**, 10959 (2020).
8. Ceylan, G., Herzog, M. H. & Pascucci, D. Serial dependence does not originate from low-level visual processing. *Cognition* **212**, 104709 (2021).
9. Fischer, C., et al. Context information supports serial dependence of multiple visual objects across memory episodes. *Nat. Commun.* **11**, 1932 (2020).
10. Moon, J. & Kwon, O.-S. Attractive and repulsive effects of sensory history concurrently shape visual perception. *BMC Biol.* **20**, 247 (2022).
11. Pascucci, D. et al. Laws of concatenated perception: vision goes for novelty, decisions for perseverance. *PLoS Biol.* **17**, e3000144 (2019).
12. Pascucci, D. & Plomp, G. Serial dependence and representational momentum in single-trial perceptual decisions. *Sci. Rep.* **11**, 9910 (2021).
13. Tanrikulu, Ö. D., Pascucci, D. & Kristjánsson, Á. Stronger serial dependence in the depth plane than the fronto-parallel plane between realistic objects: evidence from virtual reality. *J. Vis.* **23**, 20 (2023).
14. Liberman, A., Manassi, M. & Whitney, D. Serial dependence promotes the stability of perceived emotional expression depending on face similarity. *Atten. Percept. Psychophys.* **80**, 1461–1473 (2018).
15. Liberman, A. & Whitney, D. The serial dependence of perceived emotional expression. *J. Vis.* **15**, 929 (2015).
16. Kim, S., Burr, D. & Alais, D. Attraction to the recent past in aesthetic judgments: a positive serial dependence for rating artwork. *J. Vis.* **19**, 19 (2019).
17. Stern, Y., Ben-Yehuda, I., Koren, D., Zaidel, A. & Salomon, R. The dynamic boundaries of the self: serial dependence in the sense of agency. *Cortex* **152**, 109–121 (2022).
18. Taubert, J., Van der Burg, E. & Alais, D. Love at second sight: sequential dependence of facial attractiveness in an on-line dating paradigm. *Sci. Rep.* **6**, 22740 (2016).
19. Lõoke, M., Guérineau, C., Broseghini, A., Mongillo, P. & Marinelli, L. Visual continuum in non-human animals: serial dependence revealed in dogs. *Proc. R. Soc. B* **291**, 20240051 (2024).
20. Papadimitriou, C., Ferdoash, A. & Snyder, L. H. Ghosts in the machine: memory interference from the previous trial. *J. Neurophysiol.* **113**, 567–577 (2014).
21. Kalm, K. & Norris, D. Visual recency bias is explained by a mixture model of internal representations. *J. Vis.* **18**, 1 (2018).
22. Cicchini, G. M., Mikellidou, K. & Burr, D. The functional role of serial dependence. *Proc. R. Soc. B* **285**, 20181722 (2018).
23. van Bergen, R. S. & Jehee, J. F. Probabilistic representation in human visual cortex reflects uncertainty in serial decisions. *J. Neurosci.* **39**, 8164–8176 (2019).
24. Chetverikov, A. Demixing model: a normative explanation for inter-item biases in memory and perception. Preprint at *bioRxiv* https://doi.org/10.1101/2023.03.26.534226 (2023).
25. Bansal, S. et al. Qualitatively different delay-dependent working memory distortions in people with schizophrenia and healthy control participants. *Biol. Psychiatry Cogn. Neurosci. Neuroimaging* https://doi.org/10.1016/j.bpsc.2023.07.004 (2023).
26. Pascucci, D. et al. Intact serial dependence in schizophrenia: evidence from an orientation adjustment task. *Schizophr. Bull.* **51**, 754–764 (2024).
27. Stein, H. et al. Reduced serial dependence suggests deficits in synaptic potentiation in anti-NMDAR encephalitis and schizophrenia. *Nat. Commun.* **11**, 4250 (2020).
28. Manassi, M. & Whitney, D. Continuity fields enhance visual perception through positive serial dependence. *Nat. Rev. Psychol.* https://doi.org/10.1038/s44159-024-00297-x (2024).
29. Fritsche, M., Spaak, E. & de Lange, F. P. A Bayesian and efficient observer model explains concurrent attractive and repulsive history biases in visual perception. *Elife* **9**, e55389 (2020).
30. Ozkirli, A., Pascucci, D. & Herzog, M. H. Failure to replicate a superiority effect in crowding. *Nat. Commun.* **16**, 1637 (2025).
31. Sheehan, T. C. & Serences, J. T. Attractive serial dependence overcomes repulsive neuronal adaptation. *PLoS Biol.* **20**, e3001711 (2022).
32. Abreo, S., Gergen, A., Gupta, N. & Samaha, J. Effects of satisfying and violating expectations on serial dependence. *J. Vis.* **23**, 6 (2023).
33. Samaha, J. Data for 'Effects of satisfying and violating expectations on serial dependence'. *OSF* https://osf.io/kpjtb/ (2022).
34. Blondé, P., Kristjánsson, Á. & Pascucci, D. Tuning perception and decisions to temporal context. *iScience* https://doi.org/10.1016/j.isci.2023.108008 (2023).
35. Blondé, P. Tuning perception and decisions to temporal context. *Mendeley* https://doi.org/10.17632/TMWD9ZKMCX.1 (2023).
36. Ceylan, G. & Pascucci, D. Attractive and repulsive serial dependence: the role of task relevance, the passage of time, and the number of stimuli. *J. Vis.* **23**, 8 (2023).

37. Pascucci, D. Datasets for 'Serial dependence does not originate from low-level visual processing' Gizayet al., (2021): cognition. *Zenodo* https://doi.org/10.5281/zenodo.4632854 (2021).
38. Chetverikov, A. & Jehee, J. F. M. Motion direction is represented as a bimodal probability distribution in the human visual cortex. *Nat. Commun.* **14**, 7634 (2023).
39. Chetverikov, A. & Jehee, J. *Data Accompanying the Paper 'Motion Direction Is Represented as a Bimodal Probability Distribution in the Human Visual Cortex'* (Radboud Univ., 2023); https://doi.org/10.34973/YK4K-TP41
40. Cicchini, G. M., Mikellidou, K. & Burr, D. C. Data from: The functional role of serial dependence. *Dryad* https://doi.org/10.5061/DRYAD.8PH33S0 (2018).
41. Fischer, C. et al. Data. *OSF* https://osf.io/b7msj (2020).
42. Fritsche, M. & de Lange, F. P. The role of feature-based attention in visual serial dependence. *J. Vis.* **19**, 21 (2019).
43. Gallagher, G. K. & Benton, C. P. Stimulus uncertainty predicts serial dependence in orientation judgements. *J. Vis.* **22**, 6 (2022).
44. Benton, C. & Gallagher, G. *Noise and Serial Dependence* (Univ. Bristol, 2022); https://doi.org/10.5523/BRIS.3LF3SKKFZEN4A2AJZ1L6BV05GV
45. Geurts, L. S., Cooke, J. R., van Bergen, R. S. & Jehee, J. F. Subjective confidence reflects representation of Bayesian probability in cortex. *Nat. Hum. Behav.* **6**, 294–305 (2022).
46. Houborg, C., Kristjánsson, Á, Tanrıkulu, Ö. D. & Pascucci, D. The role of secondary features in serial dependence. *J. Vis.* **23**, 21 (2023).
47. Houborg, C., Pascucci, D., Tanrıkulu, Ö. D. & Kristjánsson, Á The effects of visual distractors on serial dependence. *J. Vis.* **23**, 1 (2023).
48. Lau, W. K. & Maus, G. W. Visual serial dependence in an audiovisual stimulus. *J. Vis.* **19**, 20 (2019).
49. Lau, W. K. & Maus, G. Related data for: Visual serial dependence in an audiovisual stimulus. *DR-NTU (Data)* https://doi.org/10.21979/N9/CBUORH (2020).
50. Moon, J. & Kwon, O.-S. Data for 'Attractive and repulsive effects of sensory history concurrently shape visual perception'. *OSF* https://osf.io/s3cx2 (2022).
51. Moon, J., Tadin, D. & Kwon, O.-S. A key role of orientation in the coding of visual motion direction. *Psychon. Bull. Rev.* **30**, 564–574 (2023).
52. Kwon, O.-S. Data for 'A key role of orientation in the coding of visual motion direction'. *OSF* https://osf.io/m6d4z (2022).
53. Ozkirli, A. & Pascucci, D. It's not the spoon that bends: internal states of the observer determine serial dependence. Preprint at *bioRxiv* https://doi.org/10.1101/2023.10.19.563128 (2023).
54. Ozkirli, A. & Pascucci, D. Dataset for 'It's not the spoon that bends: internal states of the observer determine serial dependence'. *Zenodo* https://doi.org/10.5281/zenodo.11187228 (2024).
55. Pascucci, D. Intact serial dependence in schizophrenia: evidence from an orientation adjustment task (version 1). *Zenodo* https://doi.org/10.1093/schbul/sbae106 (2024).
56. Sadil, P., Cowell, R. A. & Huber, D. E. The push-pull of serial dependence effects: attraction to the prior response and repulsion from the prior stimulus. *Psychon. Bull. Rev.* **31**, 259–273 (2024).
57. Samaha, J., Switzky, M. & Postle, B. R. Confidence boosts serial dependence in orientation estimation. *J. Vis.* **19**, 25 (2019).
58. Samaha, J., Switzky, M. & Postle, B. R. Data for 'Confidence boosts serial dependence in orientation estimation'. *OSF* https://osf.io/6uczk/ (2019).
59. Houborg, C., Pascucci, D., Tanrikulu, Ö. D. & Kristjánsson, Á. The effects of visual distractors on serial dependence. *Zenodo* https://doi.org/10.5281/zenodo.7940512 (2023).
60. Moscoso, P. A. M., Burr, D. C. & Cicchini, G. M. Serial dependence improves performance and biases confidence-based decisions. *J. Vis.* **23**, 5 (2023).
61. Stewart, N., Brown, G. D. A. & Chater, N. Absolute identification by relative judgment. *Psychol. Rev.* **112**, 881–911 (2005).
62. Fritsche, M., Mostert, P. & de Lange, F. P. Opposite effects of recent history on perception and decision. *Curr. Biol.* **27**, 590–595 (2017).
63. Dragoi, V., Sharma, J., Miller, E. K. & Sur, M. Dynamics of neuronal sensitivity in visual cortex and local feature discrimination. *Nat. Neurosci.* **5**, 883–891 (2002).
64. Tiurina, N. A., Markov, Y., Choung, O.-H., Herzog, M. H. & Pascucci, D. Unlocking crowding by ensemble statistics. *Curr. Biol.* **32**, 4975–4981.e3 (2022).
65. Whitney, D. & Levi, D. M. Visual crowding: a fundamental limit on conscious perception and object recognition. *Trends Cogn. Sci.* **15**, 160–168 (2011).
66. Jonides, J. & Nee, D. E. Brain mechanisms of proactive interference in working memory. *Neuroscience* **139**, 181–193 (2006).
67. Makovski, T. & Jiang, Y. V. Proactive interference from items previously stored in visual working memory. *Mem. Cogn.* **36**, 43–52 (2008).
68. Cicchini, G. M., Mikellidou, K. & Burr, D. C. Serial dependence in perception. *Annu. Rev. Psychol.* **75**, 129–154 (2024).
69. Cicchini, G. M., D'Errico, G. & Burr, D. C. Crowding results from optimal integration of visual targets with contextual information. *Nat. Commun.* **13**, 5741 (2022).
70. Glen, J. C. & Dakin, S. C. Orientation-crowding within contours. *J. Vis.* **13**, 14 (2013).
71. Livne, T. & Sagi, D. Multiple levels of orientation anisotropy in crowding with Gabor flankers. *J. Vis.* **11**, 18 (2011).
72. Solomon, J. A., Felisberti, F. M. & Morgan, M. J. Crowding and the tilt illusion: toward a unified account. *J. Vis.* **4**, 9 (2004).
73. Cicchini, G. M., D'Errico, G. & Burr, D. C. Reply to: Failure to replicate a superiority effect in crowding. *Nat. Commun.* **16**, 1638 (2025).
74. Barbosa, J. et al. Interplay between persistent activity and activity-silent dynamics in the prefrontal cortex underlies serial biases in working memory. *Nat. Neurosci.* **23**, 1016–1024 (2020).
75. Ernst, M. O. & Banks, M. S. Humans integrate visual and haptic information in a statistically optimal fashion. *Nature* **415**, 429–433 (2002).
76. Ufer, C. & Blank, H. Opposing serial effects of stimulus and choice in speech perception scale with context variability. *iScience* **27**, 110611 (2024).
77. Schwetlick, L. & Herzog, M. H. Visual crowding. *Annu. Rev. Vis. Sci.* https://doi.org/10.1146/annurev-vision-110423-024409 (2025).
78. MATLAB version R2023b. https://www.mathworks.com (The MathWorks Inc., 2023).
79. Geisler, W. S. Motion streaks provide a spatial code for motion direction. *Nature* **400**, 65–69 (1999).
80. Manassi, M., Liberman, A., Kosovicheva, A., Zhang, K. & Whitney, D. Serial dependence in position occurs at the time of perception. *Psychon. Bull. Rev.* **25**, 2245–2253 (2018).
81. Chetverikov, A. circhelp: circular analyses helper functions. *GitHub* https://github.com/achetverikov/circhelp/releases/tag/v1.1 (2024).
82. van Bergen, R. S., Ji Ma, W., Pratte, M. S. & Jehee, J. F. M. Sensory uncertainty decoded from visual cortex predicts behavior. *Nat. Neurosci.* **18**, 1728–1730 (2015).

Acknowledgements

We thank all the researchers who have shared their data directly or made it publicly available. Data from three studies were provided by the Radboud University, Nijmegen, the Netherlands. This work was supported by the Swiss National Science Foundation (SNSF) through the Ambizione Grant 'Serial Dependence in Perception and Decision Making' (D.P.; grant numbers PZ00P1_179988 and PZ00P1_179988/2) and finalized with additional support from the SNSF Starting Grant

(D.P.; TMSGI1_218247). The funders had no role in study design, data collection and analysis, decision to publish or preparation of the manuscript.

Author contributions

A.O.: conceptualization, data collection, investigation, analysis, and writing—original draft, review and editing. A.C.: conceptualization, data collection, analysis, and writing—review and editing. D.P.: conceptualization, data collection, investigation, analysis, writing—review and editing, funding acquisition and supervision.

Competing interests

The authors declare no competing interests.

Additional information

Supplementary information The online version contains supplementary material available at https://doi.org/10.1038/s41562-025-02362-8.

Correspondence and requests for materials should be addressed to Ayberk Ozkirli.

Peer review information *Nature Human Behaviour* thanks Matthias Fritsche, Huihui Zhang and the other, anonymous, reviewer(s) for their contribution to the peer review of this work. Peer reviewer reports are available.

nature portfolio

Corresponding author(s): Ayberk Ozkirli

Last updated by author(s): 2025/10/09

Reporting Summary

Nature Portfolio wishes to improve the reproducibility of the work that we publish. This form provides structure for consistency and transparency in reporting. For further information on Nature Portfolio policies, see our Editorial Policies and the Editorial Policy Checklist.

Statistics

For all statistical analyses, confirm that the following items are present in the figure legend, table legend, main text, or Methods section.

n/a	Confirmed	
☐	☒	The exact sample size (*n*) for each experimental group/condition, given as a discrete number and unit of measurement
☐	☒	A statement on whether measurements were taken from distinct samples or whether the same sample was measured repeatedly
☐	☒	The statistical test(s) used AND whether they are one- or two-sided *Only common tests should be described solely by name; describe more complex techniques in the Methods section.*
☐	☒	A description of all covariates tested
☒	☐	A description of any assumptions or corrections, such as tests of normality and adjustment for multiple comparisons
☐	☒	A full description of the statistical parameters including central tendency (e.g. means) or other basic estimates (e.g. regression coefficient) AND variation (e.g. standard deviation) or associated estimates of uncertainty (e.g. confidence intervals)
☐	☒	For null hypothesis testing, the test statistic (e.g. *F*, *t*, *r*) with confidence intervals, effect sizes, degrees of freedom and *P* value noted *Give P values as exact values whenever suitable.*
☒	☐	For Bayesian analysis, information on the choice of priors and Markov chain Monte Carlo settings
☐	☒	For hierarchical and complex designs, identification of the appropriate level for tests and full reporting of outcomes
☒	☐	Estimates of effect sizes (e.g. Cohen's *d*, Pearson's *r*), indicating how they were calculated

Our web collection on statistics for biologists contains articles on many of the points above.

Software and code

Policy information about availability of computer code

Data collection	We compiled datasets from published work, not applicable.
Data analysis	Performed on MATLAB 2023b. Code is accessible on https://github.com/aozkirli/Large-scale-mega-analysis-on-serial-dependence/tree/main

For manuscripts utilizing custom algorithms or software that are central to the research but not yet described in published literature, software must be made available to editors and reviewers. We strongly encourage code deposition in a community repository (e.g. GitHub). See the Nature Portfolio guidelines for submitting code & software for further information.

Data

Policy information about availability of data

All manuscripts must include a data availability statement. This statement should provide the following information, where applicable:

- Accession codes, unique identifiers, or web links for publicly available datasets
- A description of any restrictions on data availability
- For clinical datasets or third party data, please ensure that the statement adheres to our policy

We compiled datasets from published work. For the original raw data, we refer the readers to the referenced studies.
We are in the process of getting the permissions for data resharing (compiled standardized format of original data)

Research involving human participants, their data, or biological material

Policy information about studies with human participants or human data. See also policy information about sex, gender (identity/presentation), and sexual orientation and race, ethnicity and racism.

Reporting on sex and gender	not relevant to the research question, we do not have this data saved anywhere.
Reporting on race, ethnicity, or other socially relevant groupings	not relevant to the research question, we do not have this data saved anywhere.
Population characteristics	not relevant to the research question, we do not have this data saved anywhere.
Recruitment	the datasets we compiled were already collected by different people
Ethics oversight	the datasets we compiled were already collected by different people

Note that full information on the approval of the study protocol must also be provided in the manuscript.

Field-specific reporting

Please select the one below that is the best fit for your research. If you are not sure, read the appropriate sections before making your selection.

☒ Life sciences ☐ Behavioural & social sciences ☐ Ecological, evolutionary & environmental sciences

For a reference copy of the document with all sections, see nature.com/documents/nr-reporting-summary-flat.pdf

Life sciences study design

All studies must disclose on these points even when the disclosure is negative.

Sample size	We conducted a search on PubMed using the keyword "serial dependence" for studies published between 2014 (from the initial study of Fischer and Whitney) and 2024. Studies were selected based on the following criteria: 1. Single-trial data publicly available online, 2. Adjustment tasks involving orientation or motion stimuli with circular responses (e.g., participants reproducing orientation of a Gabor patch or motion direction of dot clouds), 3. Trial-by-trial orientation or motion direction changes (Δ) covering 0 to ±90°, using uniform/randomly determined trial-by-trial changes in Δ.
Data exclusions	If a participant did not have valid trials, or if the trials were identified as outliers as described in the manuscript
Replication	We have confirmed our results with different methods of analyses, as well as a larger sample size compared to the initial version of the manuscript
Randomization	The datasets we analyze are coming from all around the world, with different paradigms but with the same adjustment task. Furthermore, our main effect of interest is a within-subject/fixed-effect.
Blinding	N/A. This is a large-scale analysis of existing datasets.

Reporting for specific materials, systems and methods

We require information from authors about some types of materials, experimental systems and methods used in many studies. Here, indicate whether each material, system or method listed is relevant to your study. If you are not sure if a list item applies to your research, read the appropriate section before selecting a response.

Materials & experimental systems

n/a	Involved in the study
☒	☐ Antibodies
☒	☐ Eukaryotic cell lines
☒	☐ Palaeontology and archaeology
☒	☐ Animals and other organisms
☒	☐ Clinical data
☒	☐ Dual use research of concern
☒	☐ Plants

Methods

n/a	Involved in the study
☒	☐ ChIP-seq
☒	☐ Flow cytometry
☒	☐ MRI-based neuroimaging

Plants

Seed stocks	N/A
Novel plant genotypes	N/A
Authentication	N/A

Terms and Conditions

Springer Nature journal content, brought to you courtesy of Springer Nature Customer Service Center GmbH (“Springer Nature”).
Springer Nature supports a reasonable amount of sharing of research papers by authors, subscribers and authorised users (“Users”), for small-scale personal, non-commercial use provided that all copyright, trade and service marks and other proprietary notices are maintained. By accessing, sharing, receiving or otherwise using the Springer Nature journal content you agree to these terms of use (“Terms”). For these purposes, Springer Nature considers academic use (by researchers and students) to be non-commercial.
These Terms are supplementary and will apply in addition to any applicable website terms and conditions, a relevant site licence or a personal subscription. These Terms will prevail over any conflict or ambiguity with regards to the relevant terms, a site licence or a personal subscription (to the extent of the conflict or ambiguity only). For Creative Commons-licensed articles, the terms of the Creative Commons license used will apply.
We collect and use personal data to provide access to the Springer Nature journal content. We may also use these personal data internally within ResearchGate and Springer Nature and as agreed share it, in an anonymised way, for purposes of tracking, analysis and reporting. We will not otherwise disclose your personal data outside the ResearchGate or the Springer Nature group of companies unless we have your permission as detailed in the Privacy Policy.
While Users may use the Springer Nature journal content for small scale, personal non-commercial use, it is important to note that Users may not:

1. use such content for the purpose of providing other users with access on a regular or large scale basis or as a means to circumvent access control;
2. use such content where to do so would be considered a criminal or statutory offence in any jurisdiction, or gives rise to civil liability, or is otherwise unlawful;
3. falsely or misleadingly imply or suggest endorsement, approval , sponsorship, or association unless explicitly agreed to by Springer Nature in writing;
4. use bots or other automated methods to access the content or redirect messages
5. override any security feature or exclusionary protocol; or
6. share the content in order to create substitute for Springer Nature products or services or a systematic database of Springer Nature journal content.

In line with the restriction against commercial use, Springer Nature does not permit the creation of a product or service that creates revenue, royalties, rent or income from our content or its inclusion as part of a paid for service or for other commercial gain. Springer Nature journal content cannot be used for inter-library loans and librarians may not upload Springer Nature journal content on a large scale into their, or any other, institutional repository.
These terms of use are reviewed regularly and may be amended at any time. Springer Nature is not obligated to publish any information or content on this website and may remove it or features or functionality at our sole discretion, at any time with or without notice. Springer Nature may revoke this licence to you at any time and remove access to any copies of the Springer Nature journal content which have been saved.
To the fullest extent permitted by law, Springer Nature makes no warranties, representations or guarantees to Users, either express or implied with respect to the Springer nature journal content and all parties disclaim and waive any implied warranties or warranties imposed by law, including merchantability or fitness for any particular purpose.
Please note that these rights do not automatically extend to content, data or other material published by Springer Nature that may be licensed from third parties.
If you would like to use or distribute our Springer Nature journal content to a wider audience or on a regular basis or in any other manner not expressly permitted by these Terms, please contact Springer Nature at

onlineservice@springernature.com